Hydrol. Earth Syst. Sci., 15, 3741–3750, 2011
www.hydrol-earth-syst-sci.net/15/3741/2011/
doi:10.5194/hess-15-3741-2011

Hydrology and Earth System Sciences

Classifying low flow hydrological regimes at a regional scale

M. J. Kirkby[1], F. Gallart[2], T. R. Kjeldsen[3], B. J. Irvine[1], J. Froebrich[4], A. Lo Porto[5], A. De Girolamo[5], and the MIRAGE team[6]

[1]School of Geography, University of Leeds, UK
[2]Surface Hydrology and Erosion Group, Geosciences Department Institute of Environmental Assessment and Water Research (IDÆA), CSIC Barcelona, Spain
[3]Centre for Ecology & Hydrology (CEH), Wallingford, UK
[4]Centre for Water and Climate (CWK), Integrated Water Resources Management, Alterra, Wageningen, The Netherlands
[5]Water Research Institute IRSA-CNR, Bari, Italy
[6]MIRAGE project (Mediterranean Intermittent River ManAGEment): 7th EU Framework Programme, coordinated by J. Froebrich, Centre for Water and Climate (CWK), Integrated Water Resources Management, Alterra, Wageningen, The Netherlands

Received: 25 March 2011 – Published in Hydrol. Earth Syst. Sci. Discuss.: 29 April 2011
Revised: 22 November 2011 – Accepted: 30 November 2011 – Published: 19 December 2011

Abstract. The paper uses a simple water balance model that partitions the precipitation between actual evapotranspiration, quick flow and delayed flow, and has sufficient complexity to capture the essence of climate and vegetation controls on this partitioning. Using this model, monthly flow duration curves have been constructed from climate data across Europe to address the relative frequency of ecologically critical low flow stages in semi-arid rivers, when flow commonly persists only in disconnected pools in the river bed. The hydrological model is based on a dynamic partitioning of precipitation to estimate water available for evapotranspiration and plant growth and for residual runoff. The duration curve for monthly flows has then been analysed to give an estimate of bankfull flow based on recurrence interval. Arguing from observed ratios of cross-sectional areas at flood and low flows, hydraulic geometry suggests that disconnected flow under "pool" conditions is approximately 0.1 % of bankfull flow. Flow duration curves define a measure of bankfull discharge on the basis of frequency. The corresponding frequency for pools is then read from the duration curve, using this (0.1 %) ratio to estimate pool discharge from bank full discharge. The flow duration curve then provides an estimate of the frequency of poorly connected pool conditions, corresponding to this discharge, that constrain survival of river-dwelling arthropods and fish. The methodology has here been applied across Europe at 15 km resolution, and the potential is demonstrated for applying the methodology under alternative climatic scenarios.

Correspondence to: M. J. Kirkby
(m.j.kirkby@leeds.ac.uk)

1 Introduction

Many of our hopes (Sivapalan et al., 2003) of providing a basis for making predictions in ungauged drainage basins have stalled on the unexplained dissimilarities of apparently similar basins. Here we focus on the impact of climatic inputs on the hydrologic responses of catchments, paying particular attention to their low flow characteristics and how these are controlled by the seasonality of climate, the response of vegetation cover and the interactions with evapotranspiration and runoff throughout the year. This has been done by applying a relatively simple and stable water balance model, but one that is able to explicitly incorporate the main dynamic interactions with climate and vegetation at regional scales. Using gridded climate data as input, the model partitions precipitation to provide 50-yr synthetic time series for runoff which are analysed here through duration curves. It is thought that differences in monthly flow duration curves, analysed here,

can provide one tool for looking at and classifying the characteristic signatures of climate and the contrasting hydrological regimes that are driven by climatic differences. By looking for major differences across a wide range of catchments, we deliberately focus on the climatic signal that distinguishes between, for example, snow-dominated, humid and semi-arid regimes. Although unusual in being applied to monthly flows, the methods of duration flow analysis follow those recommended by Vogel and Fennessey (1994), representing the flow duration curves as log normal/probability plots as recommended by Searcy (1959).

Empirical work in Mediterranean catchments has suggested (e.g. Bonada et al., 2008; Gallart et al., 2011) that monthly flow duration curves are a valuable empirical tool for assessing the frequency of ecologically critical conditions in temporary streams. Preliminary work suggested that most of the low-flow signal in monthly duration curves could be generated using monthly climatic inputs, augmented with some information on the frequency of daily rainfall events in each month, thus opening up a much wider range of available data for analysis.

We take a very simple but rich hydrological model, focussing on monthly time steps with a superimposed distribution of daily storm rainfalls, to generate monthly flow duration curves from climatic data. At this time resolution, routing and quickflow responses play a minor part except in very large catchments ($>10^5$ km^2) so that the appropriate hydrological model is one dominated by recession behaviour. Our intention has been to parameterise this model to reflect the indirect effects of climatic differences, notably through vegetation. This approach provides a simplified physical model, building on the approach of Yokoo et al. (2008, 2011). The key differences here are in a more explicit recognition of the role of vegetation, which is set to grow in a simplified sense as part of the explicit partitioning of precipitation between overland flow, subsurface flow and evapotranspiration. On the other hand, the treatment of topographic variation is much simpler than that developed by Reggiani and Sivapalan (2000). Although the methods proposed here use statistical distributions for monthly and daily precipitation and other climate variables, they are less reliant on the statistical forms of output hydrographs than the work of Muneepeerakul et al. (2010) and Botter et al. (2009).

The work reported here focuses on low flow characteristics in semi-arid catchments with intermittently flowing streams, particularly when flow is spatially discontinuous and/or confined to disconnected pools. We are looking for regional patterns that will help define areas with different types of hydrological response in order to guide the management of non-permanent water bodies, and provide criteria of good ecological status where surface flow is occasionally to frequently absent. We are therefore attempting to model broad regional patterns in the frequency of these "pool" conditions, and examine how this frequency varies through the year. At present the approach is exploratory, proposing principles to apply rather than providing definitive conclusions, but the method is seen as having the potential to address the quality of ecological services for a range of low flow conditions, across gradients of climate, geology and human impacts.

The meteorological data is mainly from the Climatic Research Unit (CRU) (New et al., 2002; Mitchell et al., 2003) interpolated average data for a spatial grid of 10 min of arc (approximately 15 km), so that simulations are generated for source areas of about 200 km^2. These data are used to generate 50-yr synthetic climate records without trends. Potential evapotranspiration (E-T) is not included in these data, and has been estimated using the Hargreaves (Hargreaves and Samani, 1982) method, based on incoming solar radiation and temperature. The core of the hydrological model is designed to partition precipitation into the components of infiltration excess and saturation excess overland flow, subsurface flow and actual E-T. Actual and potential E-T are then used to interactively estimate uncultivated plant cover, vegetation biomass, soil organic matter biomass and runoff thresholds. The model is spun up for five years to stabilise the hydrology and then run for the 50-yr synthetic period to generate a monthly flow duration curve.

Although there are many local factors that influence hydrological response, including the presence of aquifers, variations in soil properties, imposed land use and water abstractions or return of treated wastewater, these have not been incorporated into the model presented here, allowing only broad patterns of difference to emerge that are related to climatic differences and their impact on the hydrological regimes. The model has been developed in the context of the EU FP7 MIRAGE (**M**editerranean **I**ntermittent **R**iver Man**AGE**ment) project, on water management in southern Europe, so that the examples used largely reflect concern with ecological status of temporary rivers, which is intimately linked to the presence or absence of disconnected or zero surface flow during the summer period. The MIRAGE project aims to provide a better assessment of ecological status for non-permanent streams in the Mediterranean area. Using thematic investigations in different river basins, the project is helping to develop exemplary River Basin Management Plans for two basins in Greece and Italy as a means of supporting the applicability of the EU Water Framework Directive for temporary streams, to establish generic principles for the development of Integrated Water Resources Management in the Circum-Mediterranean region, and to place the case studies into their broader regional setting. The work reported here is a contribution to the last approach.

2 Construction of synthetic climate time series

The CRU European and Global 10-min databases (New et al., 2002; Mitchell et al., 2003) contain averages for monthly total precipitation and its standard deviation, and number of rain days per month. They also contain data for temperatures

and mean values of vapour pressure or relative humidity. The European data base also contains year by year monthly values for 1901–2000, and these data are sufficient to estimate monthly potential E-T, using the Hargreaves method (Hargreaves and Samani, 1982), for each month, and consequently mean and standard deviation for each month. This method estimates top of atmosphere radiation from latitude, and air temperature to modify this to make some correction for cloudiness. Additional ERA-40 data have been added (BADC) for the coefficient of variation of rain on rain-days, averaged for the same spatial grid.

These data have then been used to define distributions, most importantly for monthly rainfalls but also for potential evapotranspiration and temperature, and a 50-yr monthly time series has been generated by drawing independent samples from these distributions. Monthly rainfall total has been drawn from a gamma distribution defined by the monthly mean and standard deviation. The gamma distribution has the requisite characteristics of having no negative values and finite moments, and has been tested in a number of contexts for rainfall data (e.g. McSweeney, 2007; Kirkby et al., 2008). The number of rain days has been adjusted from the mean value by the square root of the ratio of monthly rainfall to average monthly rainfall. In this way, months with higher than average rainfall are assumed to partition this between increases in number of rain days and mean rain per rain day. The coefficient of variation for rain-days has been kept constant at the average monthly value. Monthly potential E-T has been drawn independently at random from a normal distribution. Figure 1 shows one visualisation of a simulated set of data for an example series, near Foggia, Apulia. The web of lines, linking successive monthly values to indicate annual cycles, shows the relationship between precipitation and temperature for every month of the 50 yr period. It shows the wide variation from year to year in comparison with the mean monthly behaviour, and the variable seasonal switching common in Mediterranean areas between seasons in which precipitation is greater than or less than potential evapotranspiration. The other lines show the monthly averages for precipitation, and the mean monthly potential E-T, also plotted against mean monthly temperature. It can be seen that in this Mediterranean climate, rainfall generally exceeds potential E-T during the winter period and is less that potential E-T during the summer, although with substantial year to year variations. This pattern realistically reflects long term observed data, although it has not yet been fully tested with respect to autocorrelation.

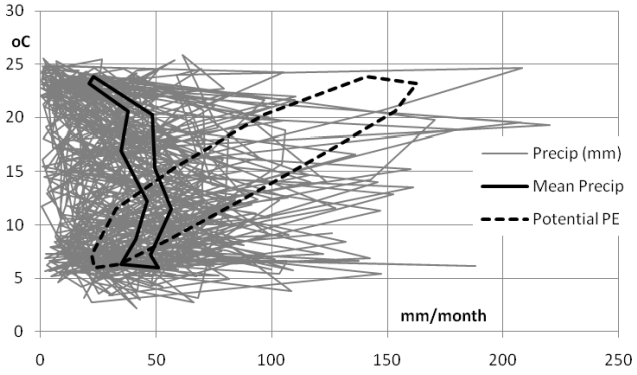

Fig. 1. Example of 50-yr synthetic climate realisation for the Celone catchment, near Foggia.

3 Structure of hydrological model

The hydrological model is designed to partition precipitation into its components (Fig. 2), and is a simplified version of that used in the PESERA (Pan European Soil ERosion Assessment) regional soil erosion model (Kirkby et al., 2008). The key elements of the model estimate actual E-T and the elements of runoff in relation to precipitation and soil moisture. The set of model equations are summarized in the Appendix.

For actual E-T (Box A in Fig. 2), some water is taken directly from rainfall for rain days, limited by daily evaporative demand in relation to the distribution of available daily rain amounts. If the evaporative demand has not been satisfied from this near-surface water, vapour is additionally drawn from the subsurface saturated zone, balancing changes in water deficit against percolating residual rainfall, drainage and evaporative demand from vegetated and bare fractions of the surface, as a function of deficit and rooting depth. This allows actual E-T to follow potential E-T in wet conditions, and to draw down soil moisture in dry conditions, while never exceeding either potential E-T or precipitation over the water year.

The runoff components represent infiltration excess and saturation excess processes. Infiltration excess overland flow is estimated by summing the daily rainfalls in excess of a runoff threshold (Box B in Fig. 2). This methodology is inherited from the PESERA model, where it has provided the basis for estimating soil erosion based on the month by month distribution of these runoff amounts. Although there are limitations in using daily rainfalls, this simplification has been used as a compromise between our understanding of the processes and the availability of regional data at finer time resolutions. After allowing for losses or gains from snowfall or snowmelt, from infiltration excess overland flow and from near-surface evaporation, the residual net rainfall percolates to a saturated sub-surface zone. The saturation deficit is updated for fractions (normally one fifth) of a month, balancing percolation against losses due to drainage (as lateral subsurface flow) and E-T from the saturated zone. Actual subsurface E-T is estimated from the available water and evaporative demand, using a modification of the Budyko approach (Pike, 1964; Arora, 2002) . These estimated are made directly for monthly totals. Subsurface drainage is estimated using the most basic version of TOPmodel (Beven

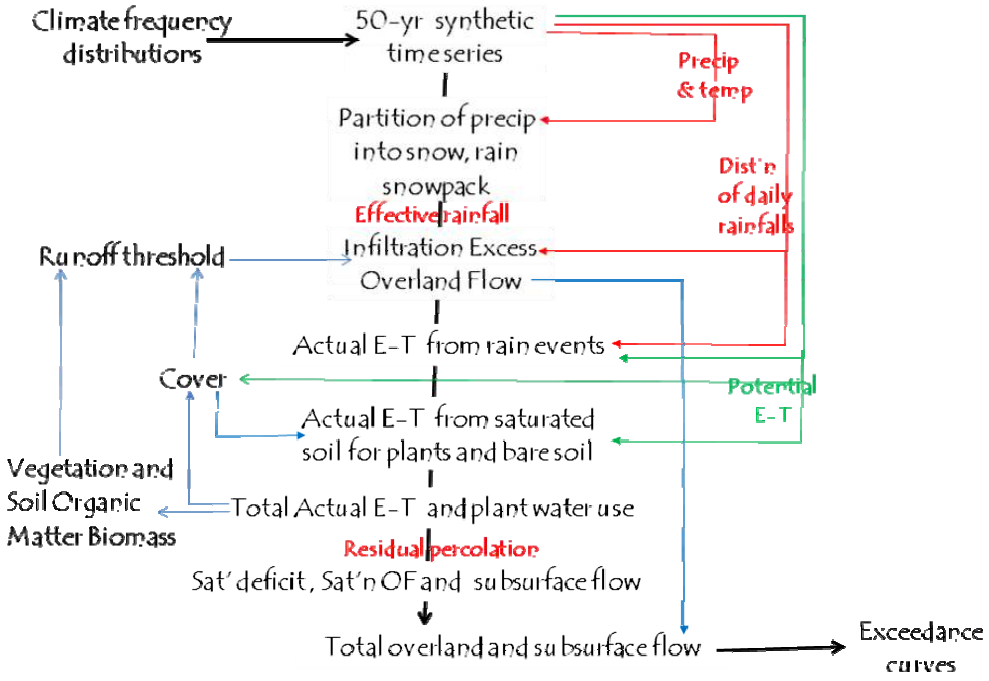

Fig. 2. Schematic for hydrological model.

and Kirkby, 1979), in which lateral flow decreases exponentially with increases in saturation deficit. Where saturation deficit falls to zero, a third component of runoff, as saturation excess overland flow, is also estimated. No over-sampling is used to estimate these components, and topography is implicitly represented by the single parameter j_0 (Appendix, Eq. 5). The monthly calculation is sub-divided into several steps to ensure computational stability.

Input is taken monthly from the synthetic climate time series. First precipitation is partitioned into rain and snow, using an estimate of the fraction of the month during which temperature is below freezing. The snowpack gains from snowfall, and loses snowmelt, estimated from a day-degree model to give an effective rainfall. Infiltration excess overland flow is estimated from a runoff threshold that varies in response to vegetation cover and soil organic matter. The distribution of daily rainfalls for each month (taken directly from the gridded interpolated climate data) is fitted to a Gamma distribution and the overland flow estimated by summing over the frequency distribution of rainfalls in excess of the threshold. The distribution of daily rainfalls is also used to estimate the amount of water that is available for near-surface E-T. (Appendix, Eq. 1)

The residual rainfall percolates into the soil, and the month is subdivided to update the saturation deficit in stages to maintain computational stability, allowing for sub-surface flow and saturation excess overland flow when appropriate. There is also a loss by further E-T from the saturated zone, calculated separately for vegetated and bare areas. Combining these components provides an estimate for total actual E-T (Appendix, Eqs. 2–4), plant water use (pro-rated to cover) and the several components of runoff by overland and sub-surface pathways.

Plant water use is then used to estimate vegetation and soil organic matter biomass, assuming that gross primary productivity is directly proportional to the transpiration stream passing through the plant (Leith and Whittaker, 1975). GPP, respiration and leaf-fall were updated monthly; and leaf fall budgeted against decomposition to "grow" living biomass and soil organic matter biomass in the model. Since water use is partly dependent on vegetation properties as crown cover and biomass develop, there is a dynamic interaction between biomass and water use that determines both as a function of climate. Although a transient model might be desirable, it was recognised that times for equilibration, particularly for organic matter in potentially saturated environments, might be excessive, so that biomass was first calculated for the equilibrium conditions in which the distribution of average conditions led to a repeated annual cycle, and then updated over the time series realisation period to allow for minor changes in response to climate variability. Finally cover and biomass were used to update the runoff threshold, providing a dynamic link between overland flow runoff and vegetation in response to the prevailing climate.

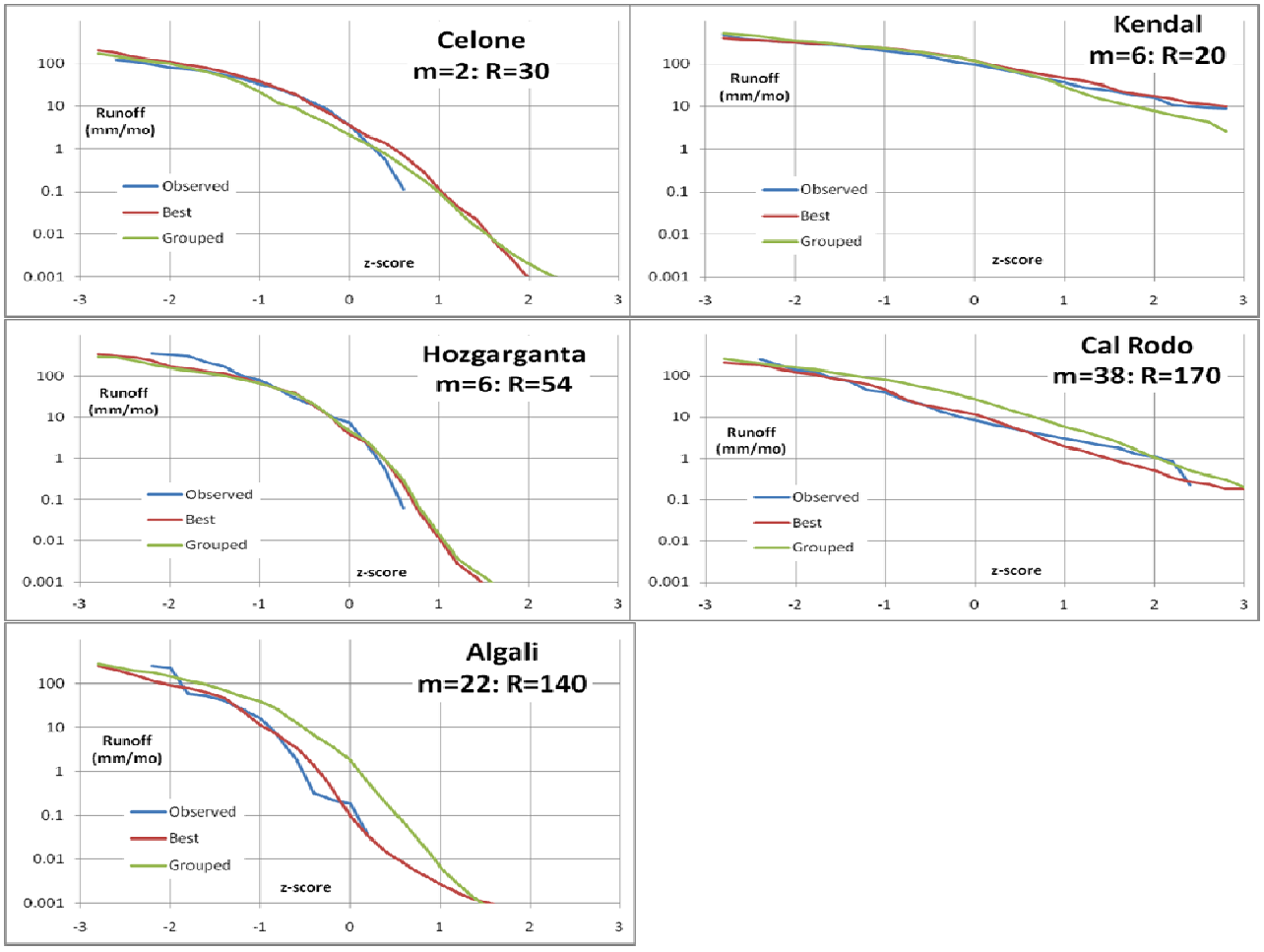

Fig. 3. Flow duration curves for the five test catchments. Each graph shows the observed data, the individual best fit model and the grouped best fit model. *R* and *m* refer to TOPModel parameters.

4 Flow duration curves and other indicator tools

The model is based on runoff generation from source areas, and assumes that all runoff pathways contribute to stream flow downstream. Flow duration curves were generated from the combined total runoff contributions for each month, providing a basis that, in our experience, could be most reliably compared with observed data. The simulated monthly runoff data were ranked and presented as a plot of log(monthly discharge) against probability of exceedance, plotted on a probability scale or z-score, so that a log-normal distribution of discharges appears as a straight line. Since, we wish to analyse the frequency of low flow conditions, we have preferred to use the complete synthetic record, rather that partition it from the ouset on the basis of dry periods, as has been proposed by Viola et al. (2011). Examples are shown in Fig. 3.

Five catchments with good hydrological records have been chosen across a range of environments to examine the response of the flow duration curves to climate. Table 1 summarizes their characteristics, showing their position, catchment area, precipitation, runoff and estimated potential E-T. It can be seen that the catchments range from semi arid, with precipitation less than half potential E-T, to humid with precipitation exceeding potential E-T, and with a range of seasonality.

These test catchments have been used to test whether the hydrological model is able to distinguish broad differences in flow duration curve characteristics with a global calibration, but without individual calibration for each site.

The model is driven by three significantly changeable parameters. The first of these is the TOPmodel *m* parameter, which scales the rate at which subsurface drainage decreases as saturation deficit increases, and has the dimensions of depth (mm of water). High values of *m* provide some subsurface flow even at high deficits, and give long-tailed recession curves, whereas low values of *m* give flashy response, with negligible flow at high saturation deficit. The value of m scales the deficits (and implicitly depths) to which water will drain.

Table 1. Summary characteristics of catchments studied and estimated 'bankfull' discharge and 'pool' (or lower) flow frequency

Name	Latitude (°N)	Longitude (°E)	Catchment area (km^2)	Precipitation ($mm\,yr^{-1}$)	Runoff ($mm\,yr^{-1}$)	Potential evapo-transpiration	Estimated bank-full flow ($mm\,mo^{-1}$)	Estimated pool Frequency (%)
Hozgarganta, Spain	36.4	−5.4	245	699	471	1053	291	28 %
Cal Rodo, Spain	42.2	1.9	4.2	989	302	776	185	0.2 %
Algali, Portugal	39.1	−7.2	122	640	137	1170	180	73 %
Kendal, UK	54.4	−2.7	209	2064	1410	577	367	< 0.1 %
Celone San Vincenzo, Italy	41.3	15.5	86	465	178	991	160	17 %

The second control parameter is the rooting depth under vegetation, R, which is also expressed as a water deficit. Vegetation is able to extract transpiration water readily under conditions when the deficit is less than the rooting depth, and progressively less as the deficit increases. Bare soil evaporation is also allowed, but with a small (5mm) scale depth, and total transpiration loss combines bare soil and plant transpiration according to the prevailing crown and root cover.

The third parameter is the subsurface runoff at saturation, j_*. This is important for partitioning between subsurface and saturation excess overland flow, and is increasingly important as the simulation time step is reduced, but has little impact on total runoff for the monthly time steps used here. Other-constant coefficients control the rate of conversion of plant transpiration to biomass, respiration, decomposition, and fall of leaves, stems and roots. These, with their dependencies on temperature and biomass where appropriate, have been taken from values reported in the literature andpreviously used in the PESERA model (Kirkby et al., 2008).

For suitable climatic areas, the model shows three main response zones to the two primary parameters. First a zone in which rooting depth is much less than TOPmodel m. Here the response is dominated by subsurface and saturation excess overland flow, with little sensitivity to the vegetation. In humid areas, the soil is frequently close to saturation, and plant growth is unrestricted by water. In more arid areas, few of these shallow-rooted plants are able to survive. In a second zone, where rooting depth is substantially greater than TOPmodel m, the hydrology is dominated by root extraction, with minimal lateral subsurface drainage. Under humid conditions, most runoff occurs as saturation excess overland flow, while in semi-arid conditions deep-rooted plants exploit percolating storm rainfall. However, the response of the catchments investigated all lay between these extremes, in a zone where both subsurface flow and plant transpiration play a part. Where the climate is seasonal, then dry seasons are typically dominated by root extraction, and wet seasons by increased subsurface flow.

For the five test catchments, the goodness of fit of the modelled flow duration curve was estimated from the average root mean square (RMS) difference between observed and estimated log (discharge) across the range of non-zero values. To minimise inconsistencies, the same particular climate realisation was used for all parameter values, as each different realisation produces a slightly different error. Figure 4a shows an example for the Hozgarganta catchment, over the ranges $m = 2$–52 mm; $R = 10$–210 mm. It can be seen that there is a weakly defined optimum at $m = 6$ mm; $R = 54$ mm, within a trough-shaped region in which m and R increase together, maintaining moderately low values of the RMS error. Similar mappings can be made for the other catchments, and Fig. 3 shows the optimum values of m and R for each. Comparing these values, it appears that higher values of m are generally associated with higher values of R. This general relationship is implicit in the general form of the model equations and inherent model dynamics. However, this preliminary conclusion will need further testing in due course.

It is therefore suggested that a single grouped parameter set based on minimising the averaged errors for the five catchments taken together might encapsulate much of the significant climatic difference across all sites. Thus, by using a single set of parameters, robustness of model performance across sites is improved at the expense of optimal goodness-of-fit at individual sites. The model therefore uses no external soil parameters, but either globally appropriate values (for m, j_* and R), values that have been internally generated by the dynamics of the model (vegetation and organic matter biomass), or constants that have been previously tested and applied within the PESERA model (Kirkby et al., 2008).

To estimate the best grouped values, individual error maps for each site (similar to Fig. 4a) have been normalised to (RMS value – Minimum value)/(Maximum value – Minimum Value), so that each error map is linearly transformed to the range [0,1]. Figure 4b is then obtained as the average of the five normalised error maps, and itself shows a minimum, with an average of 13.4 % deviation from the individual optima. This minimum sets the grouped parameter values at $m = 6$ mm; $R = 50$ mm. An alternative criterion is, for each parameter set, to map the largest of the normalised errors for the test catchments; and select the least maximum (27 %) , a minimax solution that gives parameter values of $m = 6$ mm; $R = 60$ mm. The former values have been used, giving a minimax normalised error of 32 %.

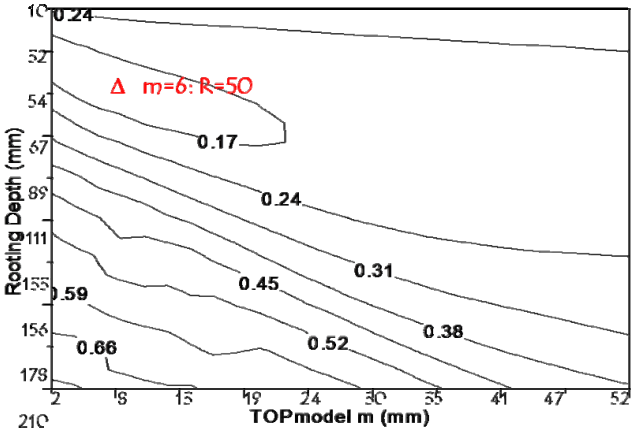

Fig. 4a. RMS mean difference between observed and simulated flow duration curves for R. Hozgarganta, S. Spain. The optimal set of model parameters are shown as Δ.

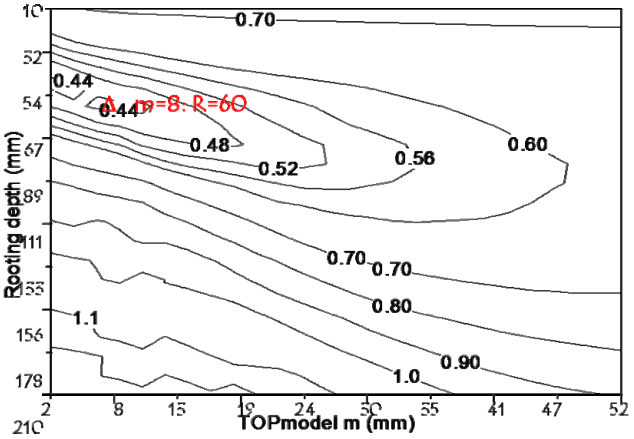

Fig. 4b. Average normalised departure averaged across five test catchments from their individual minimum RMS error. Δ shows global optimum.

For each of the five test catchments, Fig. 3 shows the flow duration curves plotted from the observed data, and with simulated curves generated with the local best fit parameter set ("Best") and the grouped set. It can be seen that differences between the three curves for each site are much smaller than the differences between the five sites, and this encourages us to use the grouped parameter values to simulate regional patterns of natural variation in the duration curves, encapsulating the main differences between areas, although inevitably providing a fit that is less good that the individual calibration for each site. It is recognised that many factors are not taken into account in this analysis, including the impact of non-natural vegetation, abstraction of water for irrigation, domestic use and industry, return of urban waste water and exchange with aquifers, particularly karst aquifers.

5 Analysis of low flow conditions from duration curves

To interpret low flow conditions for streams in different climates, we have used the concept of bank full discharge to provide a generalised measure for the dimensions of channel-forming peak flows, and have used the well known, although not necessarily totally reliable, method of associating bank full discharge with a frequency of occurrence. An exceedance with a z-score of −2.5, corresponding to a probability of 0.62 % , or 3.7 months in 50 yr. Here we are using a rarer event than that normally used to define bank full flows (1–5–10 yr Recurrence interval) to compensate for the use of monthly total flows (Leopold, 1994; Pickup and Warner, 1976), but which is still within the range of flows observed and modelled with a 50 yr synthetic climate series. This discharge is used to indicate the cross sectional area of the bank full channel. Since at-a-station discharge is approximately proportional to cross sectional area to a power, typically 0.6 (Leopold and Maddock, 1953), then reductions in discharge correspond to reductions in wetted cross-sectional area. Table 2 shows observed ratios between bank full discharges and discharges at which disconnected pools are present for a set of catchments in southern Europe studied in the MIRAGE project for which these data have been observed. Only one of these catchments is the same as the catchments listed in Table 1. The geometric mean of the listed flood to pool discharge ratios is 1100, and the median is 950. From these data it is proposed to use a discharge ratio of 1000 as an indicator of pool conditions, and this should correspond to a cross-sectional ratio of $1000^{1/0.6}$, i.e. 10^5. This then provides a discharge estimate for pool conditions, and the flow duration curve can be used to interpolate the corresponding frequency of the poorly connected pool conditions that constrain survival of river-dwelling arthropods and fish. An intermediate "riffle" stage has also been used for illustrative purposes, corresponding to a discharge ratio of $\sqrt{(1000)}$, or a cross-sectional area ratio of 300. Below this level continuous flow is anticipated, but without drowning out riffles and similar features.

Figures 5 and 6 show the regional aridity and the predicted frequency of pools under the current climate. In Fig. 5, aridity is indicated by the average number of months per year with precipitation less than 60 % of potential evapotranspiration. There is a clear north south gradient with many Mediterranean areas having more than 4.5 dry months in the summer. In Fig. 6, the model has been applied to show the frequency of "pool" conditions throughout the year. It can be seen that the forecast pattern, although identifying the same north south differences, has a much sharper concentration towards the south.

Figure 7 shows the corresponding distribution with a uniform 2 °C rise in temperature. It can be seen that the differences are small, but generally in the direction of a small reduction in the frequency of pool conditions. The temperature

Table 2. Ratios of flood to pool discharges reported for some MIRAGE catchments for which these levels have been observed.

Catchment	Area (km^2)	Runoff ($mm\,yr^{-1}$)	Flood: pool discharge ratio
Salsola-Casanova, Italy	43	107	400
Salsola-Ponte Foggia, Italy	46	85	400
Celone-S. Vincenzo, Italy	86	178	1500
Celone-Ponte Foggia, S. Severo, Italy	256	95	2000
Vrontanno, Greece	1373	23	20 000
Tordera, Spain	868	185	200

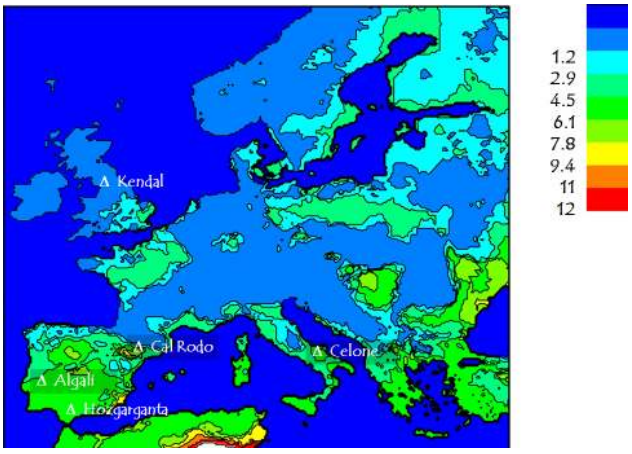

Fig. 5. Average number of months with Precipitation <0.6 Potential ET. Figure also shows location of test catchments.

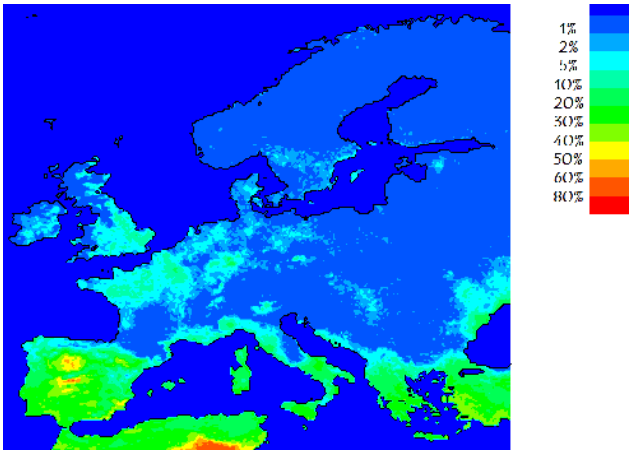

Fig. 6. Percentage of time with low flow "pool" conditions, derived from monthly duration curves for present climate.

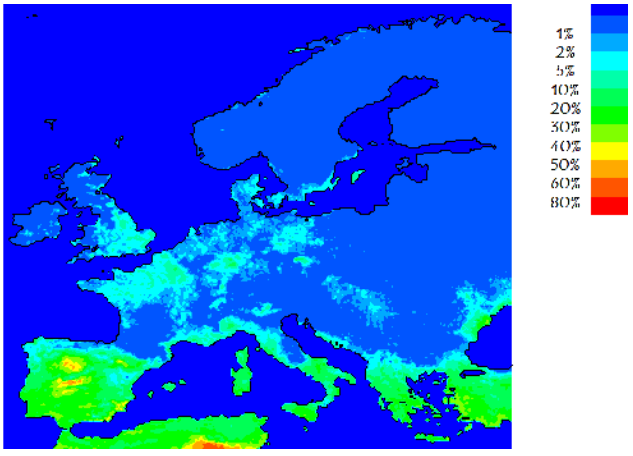

Fig. 7. Percentage of time with low flow "pool" conditions, derived from monthly duration curves with 2 °C warming.

rise increases potential E-T, and this has some effect on natural vegetation biomass, which increase where there is adequate rainfall. There is a consequent reduction in runoff, which decreases both flood and low flows. It is therefore argued that the short term impact of a step rise in temperature may be some increase in low flow (pool) frequency but that, after a period of channel adjustment, bankfull channel dimensions will decrease, partially counteracting the initial change.

Although there is substantial variability, there is a general relationship between the mean value of forecast pool frequency and the number of dry months per year, and this relationship is little changed by a 2 °C temperature rise. Figure 8 shows that this average behaviour is non-linear with a more rapid increase in pool frequency above about 4 dry months per year, which is consistent with the strong concentration apparent in Figs. 6 and 7 towards southern Europe and the Mediterranean.

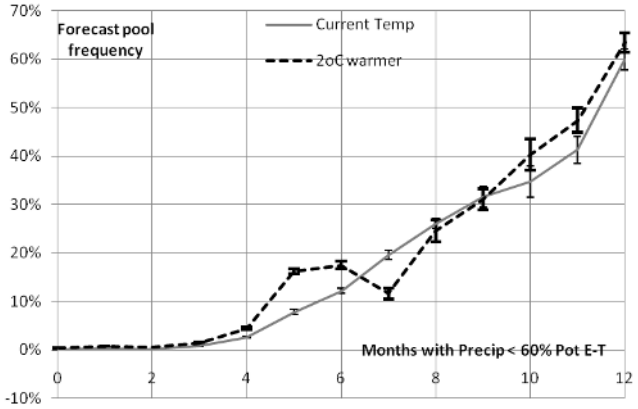

Fig. 8. Empirical relationship between forecast pool frequency and the average number of dry months (Precip < 0.6 Pot E-T) for current climate and with a 2 °C temperature rise.

6 Conclusions

The exploratory model presented shows some potential for estimating the hydrological impact of climate in time and space, containing a number of feedback paths, mainly through vegetation, that influence the partition of precipitation between evapotranspiration and runoff and so provide a dynamic response to differences in both climate and natural vegetation. The use of the monthly duration curve provides a rather stable indicator of overall behaviour, particularly at low flows. Here the analysis has focussed on the occurrence of disconnected pools at the lowest dry season flow , and it has been shown that the use of a single parameter set, calibrated against a group of sample catchments, provides a useful indication of the regional distribution of pool conditions, and one that can be applied using only climatic data, and so has the potential for application to ungauged catchments.

Appendix A

Model equations

Monthly infiltration excess overland flow is summed over distribution of daily rainfalls for which rainfall r is greater than the runoff threshold h_c.

$$q_{OF} = N \int_{h_c}^{\infty} (r - h_c) . \frac{r^{\alpha-1}}{\beta \Gamma(\alpha)} \exp\left(-\frac{r}{\beta}\right) dr \quad \text{(A1)}$$

Where N is the number of rain days, h_c is the current runoff threshold, r is the daily effective rainfall, α is the Gamma parameter = (Mean daily rainfall)/(standard deviation of rain on rain days), B is the ratio (mean rain per rain day)/α. And Γ represents the Gamma function.

Monthly near-surface evapotranspiration is similarly summed for days when effective rainfall is greater than the potential E-T demand.

$$\text{aet}_S = N \left[\int_0^e r . \frac{r^{\alpha-1}}{\beta \Gamma(\alpha)} \exp\left(-\frac{r}{\beta}\right) \mathrm{d}r + e \int_e^{\infty} \frac{r^{\alpha-1}}{\beta \Gamma(\alpha)} \exp\left(-\frac{r}{\beta}\right) dr \right] \quad \text{(A2)}$$

Where e is the lesser of daily evaporative demand or the runoff threshold, h_c .

The E-T from the saturated zone is estimated form the relationship

$$\text{aet}_d = 1 \Big/ \sqrt{\left(1/A^2 + 1/E^2\right)} \quad \text{(A3)}$$

Where the available water,

$$A = R \exp(-D/R), \quad \text{(A4)}$$

in which R is the rooting depth and D is the saturation deficit (or zero if it is negative). And E is the (residual) potential E-T demand. This subsurface E-T component is calculated separately for vegetated and bare fractions of the surface, and combined to provide the total actual E-T, and the plant water uptake.

Subsurface deficit is updated by solving the TOPmodel equations:

$$\frac{\mathrm{d}j}{\mathrm{d}t} = \frac{j.(i-j)}{m} \qquad j = j_* \exp(-D/m) \quad \text{(A5)}$$

Where j is the subsurface runoff rate, i is the net rate of percolation to the saturated zone = Net Rainfall – Overland flow – Actual E-T and m is the TOPmodel soil depth parameter. Equations (A3)–(A5) are normally solved by subdividing the month into five, progressively updating each component to its monthly total.

Cover is modified monthly, always converging towards the value $\sqrt{\frac{\text{Plant water uptake}}{\text{Potential E}-\text{T}}}$, but with 50 % inertia, and Root cover, which is taken to be more complete than surface cover, is estimated as $\surd$ (Cover). Equilibrium Plant and Soil organic matter biomass are estimated annually, from the equations:

Gross primary productivity = respiration + Leaf Fall.

Leaf Fall = SOM decomposition. Where GPP $\sim$ Plant Water Uptake, Respiration

$$\sim \exp\left(\frac{T-10}{8}\right) \quad \text{(A6)}$$

In which T is temperature in °C, Leaf fall

$$\sim \frac{V}{\log(V+1.4)} \quad \text{(A7)}$$

In which Vegetation biomass, V, is in kg m^{-2}, and

Annual decomposition

$$= \left\{\exp\left[0.05\exp(0.12T)\right] . - 1\right\} H) \quad \text{(A8)}$$

In which H is the SOM biomass. Finally the runoff threshold h_c , is estimated as

$$h_c = 10 + 40.C + 50\left[1 - \exp(-H/10)\right].C, \quad \text{(A9)}$$

Where C is the fractional crown cover.

Supplementary material related to this article is available online at: http://www.hydrol-earth-syst-sci.net/15/3741/2011/hess-15-3741-2011-supplement.pdf.

Acknowledgements. The research reported here received funding from the European Community's Seventh Framework Programme (FP7/2007-2011) under grant agreement 211732 (MIRAGE project).

Edited by: P. Claps

References

Arora, V. K.: The use of thearidity index to assess climate change effect on annual runoff, J. Hydrol., 265, 164–177, 2002.

BADC: http://badc.nerc.ac.uk/view/badc.nerc.ac.uk__ATOM__dataent_ECMWF-E40, last access: 2008, 2006.

Beven, K. J. and Kirkby, M. J.: Towards a simple, physically based, variable contributing area model of catchment hydrology, Int. Ass. Hydrol. Sci. Bull. 24, 43–69, 1979.

Bonada, N., Rieradevall, M., Dallas, H., Davis, J., Day, J., Figueroa, R., Resh, V. H., and Prat, N.: Multi-scale assessment of macroinvertebrate richness and composition in Mediterranean-climate rivers, Freshwater Biol., 53, 772–788, 2008.

Botter, G., Porporato, A., Rodriguez-Iturbe, I., and Rinaldo, A.: Nonlinear storage-discharge relations and catchment streamflow regimes, Water Resour. Rese. 45, W10427, doi:10.1029/2008WR007658, 2009.

Gallart, F., Prat, N., Brito, D., García-Roger, E., De Girolamo, A. M., Barberá, G. G., Latron, J., Llorens, J. P., Lo Porto, A., Neves, R., Tzoraki, O. , Querner, E. P., Quiñonero, J. M., Rieradevall, M., Tournoud, M. G., Nikolaidis, N. P., and Froebrich, J.: Using qualitative flow states for characterizing regimes of temporary streams: The "Aquatic States". Poster presented at IUGG conference, Melbourne July 2011, session HW13, available at: https://iugg2011.epresenter.com.au/delegate.ep#lmdl=Login;smod=Base, 2011.

Hargreaves, G. H. and Samani, Z. A.: Estimating potential evapotranspiration, ASCE J. Irrig. Drain. Div., 108, 225–230, 1982.

Kirkby, M. J., Irvine, B. J., Jones, R. J. A., Govers, G., and the PESERA team: The PESERA coarse scale erosion model for Europe: I – Model rationale and implementation, Eur. J. Soil Sci., 59, 1293–1306, 2008.

Leith, H. and Whittaker, R. H. (Ed.): Primary Productivity of the Biosphere, Ecol. Stu., V. 14, Springer-Verlag, Berlin, 1975.

Leopold, L. B.: A view of the river,Harvard University Press, Cambridge, 1994.

Leopold, L. B. and Maddock, T.: The Hydraulic Geometry of Stream Channels and Some Physiographic Implications, USGS professional Paper 252, 56 pp, 1953.

McSweeney, C. F.: Daily Rainfall Variability at Point and Areal Scales: Evaluating Simulations of Present and Future Climate, PhD thesis, April 2007, CRU, University of East Anglia, 2007.

Mitchell, T. D., Carter, T. R., Philip D. Jones, P. D., Hulme, M., and New, M.: A comprehensive set of high-resolution grids of monthly climate for Europe and the globe: the observed record (1901–2000) and 16 scenarios (2001–2100). Tyndall Centre for Climate Change Research Working Paper 55, 25 pp., 2004.

Muneepeerakul, R., Azaele, S., Botter, G., Rinaldo, A., and Rodriguez-Iturbe, I.: Daily stream flow analysis based on a two-scaled gamma pulse function, Water Resour. Res., 46, W11546, doi:10.1029/2010WR009286, 2010.

New, M., Lister, D., Hulme, M., and Makin, I.: A high resolution data set of surface climate over global land areas, Clim. Res., 21, 1–25, doi:10.3354/cr021001, 2002.

Pickup, G. and Warner, R. F.: Effects of hydrologic regime on magnitude and frequency of dominant discharge, J. Hydrol., 29, 51–75, 1976,

Pike, J. G.: The estimation of annual runoff from metorological data in a tropical climate, J. Hydrol., 2, 116–123, 1964.

Reggiania, P. and Sivapalan, M.: Conservation equations governing hillslope responses: exploring the physical basis of water balance, Water Resour. Res., 36, 845–1863, 2000.

Searcy, J. K.: Flow Duration curves, USGS Water Supply paper 1542-A, 1959.

Sivapalan, M., Takeuchi, K., Franks, S. W., Gupta, V. K., Karambiri, H., Lakshmi, V., Liang, X., McDonnell, J. J., Mendiondo, E. M., O'Connell, P. E., Oki, T., Pomeroy, J. W., Schertzer, D., Uhlenbrook, S., and Zehe, E.: IAHS decade on predictions in Ungauged Basins (PUB), 2003-2012: Shaping an exciting future for the hydrological sciences,Hydrol. Sci. J., 48, 857–880, 2003.

Viola, F., Noto, L. V., Cannarozzo, M., and La Loggia, G.: Regional flow duration curves for ungauged sites in Sicily, Hydrol. Earth Syst. Sci., 15, 323–331, 2011.

Vogel, R. M. and Fennessey, N. M.: Flow Duration Curves, I: New interpretations and confidence limits, J. Water Resour. Plan. Manag., 120, 485–504, 1994.

Yokoo, Y., Sivapalan, M., and Oki, T.: Investigating the roles of climatic seasonality and landscape characteristics o mean annula and monthly water balances, J. Hydrol., 357, 255–269, 2008.

Yokoo, Y. and Sivapalan, M.: Towards reconstruction of the flow duration curve: development of a conceptual framework with a physical basis, Hydrol. Earth Syst. Sci., 15, 2805–2819, doi:10.5194/hess-15-2805-2011, 2011.